



Beaudoin, N., Lacombe, O., Roberts, N. M.W. and Koehn, D. (2018) U-Pb dating of calcite veins reveals complex stress evolution and thrust sequence in the Bighorn Basin, Wyoming, USA. *Geology*, 46(11), pp. 1015-1018.

There may be differences between this version and the published version. You are advised to consult the publisher's version if you wish to cite from it.

<http://eprints.gla.ac.uk/169549/>

Deposited on: 7 December 2018

Enlighten – Research publications by members of the University of Glasgow_
<http://eprints.gla.ac.uk>

1 U-Pb dating of calcite veins reveals complex stress
2 evolution and thrust sequence in the Bighorn Basin,
3 **Wyoming, USA**

4 **Nicolas Beaudoin¹, Olivier Lacombe², Nick M W Roberts³, and Daniel Koehn⁴**

5 *¹Laboratoire des Fluides Complexes et leurs Réservoirs-IPRA, E2S-UPPA, Total, CNRS,*
6 *Université de Pau et des Pays de l'Adour, UMR5150 Pau, France*

7 *²Sorbonne Université, CNRS-INSU, Institut des Sciences de la Terre de Paris, ITeP*
8 *UMR 7193, F-75005 Paris, France*

9 *³NERC Isotope Geosciences Laboratory, British Geological Survey, Keyworth NG12*
10 *5GG, UK*

11 *⁴School of Geographical and Earth Sciences, University of Glasgow, Gregory, Building,*
12 *Lilybank Gardens, G12 8QQ Glasgow, UK*

13 **ABSTRACT**

14 We report U-Pb absolute ages of calcite cements from a diffuse vein network
15 documented in the Bighorn Basin (Wyoming, USA), where distinct systematic vein sets
16 developed at the front of the thin-skinned Sevier orogen, during Laramide layer-parallel
17 shortening, and during thick-skinned Laramide thrusting and folding. The U-Pb age
18 distribution illustrates: (1) an outward (eastward) transmission of Sevier orogenic stress
19 (from 89.7 ± 2.9 Ma [2σ] in the west, and from 75.3 ± 2.8 Ma in the east); and (2) an
20 inward (westward) development of Laramide-related fracturing and folding (72 ± 3.0 Ma
21 and 45.4 ± 1.8 Ma, respectively, in the east; 60.5 ± 4.6 Ma and 27.9 ± 1.1 Ma,
22 respectively, in the west), which is in accordance with the known sequence of

exhumation of the major Laramide basement arches. Our results also show that the stress related to Laramide compression first overprinted the stress related to Sevier compression in the sedimentary cover around major basement uplifts. This study highlights the utility of U-Pb calcite geochronology as a powerful tool for constraining complex sequences of deformation in orogenic forelands.

INTRODUCTION

The complex tectonic history of orogenic forelands is often reflected by equally complex fracture networks within poorly deformed or folded sedimentary strata. Systematic vein populations (and meso-scale faults, as well) are usually interpreted as resulting from local (e.g., fold-related) and/or regional (e.g., far-field stress transmission) tectonic evolution (e.g., Bergbauer and Pollard, 2004). However, absolute timing is never resolved through field-based geometrical relationships; thus, the relevance and meaning of some vein structures with respect to regional deformation can be disputable, especially in regions that underwent polyphase tectonics, with implication of different structural styles (Tavani et al., 2015). Recent progress in U-Pb dating of calcite applied to fault and vein filling has paved the way to produce more complete chronological records of deformation (Roberts and Walker, 2016; Ring and Gerdes, 2016; Nuriel et al., 2017; Hansman et al., 2018; Parrish et al., 2018). This technique opens up new exciting possibilities to better constrain how polyphase deformation and related stresses distribute in space and time during shortening in orogenic forelands.

In this study, we focus on the Sevier-Laramide Bighorn Basin (Wyoming, USA). Though Laramide basement uplifts and associated folds and faults have been extensively studied for decades (e.g., Stearns, 1971), the sequence of basement-thrust activation in

this system is still debated (Erslev, 1993), as are models accounting for the transition from thin-skinned Sevier to thick-skinned Laramide deformation (Yonkee and Weil, 2015). The sedimentary cover in the Bighorn Basin hosts a polyphase systematic vein network that recorded tectonic events encompassing the Cretaceous–early Paleocene Sevier and the Late Cretaceous–Paleogene Laramide shortening (e.g., Bellahsen et al., 2006). We apply U-Pb dating on calcite cements of these systematic vein sets in order to better constrain (1) the absolute timing of Sevier-Laramide deformation at the basin scale; and (2) the transmission and distribution of orogenic stress in a place where thin-skinned and thick-skinned styles of deformation interacted in a complex way.

GEOLOGICAL SETTING

The Bighorn Basin (Fig. 1) is part of the deformed foreland of the Sevier-Laramide orogens that formed in response to the subduction of the Farallon plate. The Sevier belt formed first as a thin-skinned wedge (i.e., basement remaining undeformed), and propagated eastward during Cretaceous to early Paleocene times in an east-west shortening direction (DeCelles, 2004). Thick-skinned Laramide deformation (i.e., involving the basement) initiated eastward by Late Cretaceous until Paleogene times with northeast-southwest-directed shortening, and overlaps with the final part of Sevier deformation (Yonkee and Weil, 2015). The mechanisms that led to basement shortening far away from the plate boundary are still debated (Yonkee and Weil, 2015). The Laramide contraction caused the inversion of preexisting faults inherited from Proterozoic extensional tectonics (Fig. 1; Marshak et al., 2000). This resulted in large basement uplifts (arches) that topographically compartmentalized the former Sevier marine foreland basin into continental, endorheic basins (Erslev, 1993; Erslev and

Rogers, 1993; Stone, 1993; DeCelles, 2004). The Bighorn Basin was subsequently isolated by three main basement arches (Fig. 1): the Bighorn Mountains to the east, the Beartooth Mountain to the northwest, and the Wind River Range to the south. The interior of the basin hosts northwest-southeast–striking, basement-cored anticlines: the Rattlesnake Mountain and Sheep Mountain–Little Sheep Mountain anticlines, that are interpreted as having developed on back-thrusts soled on the west-dipping Oregon thrust and east-dipping Rio thrust, respectively (Fig. 1C; Stanton and Erslev, 2004; Neely and Erslev, 2000);.

The exhumation and cooling history of the Laramide arches have been extensively studied by thermochronological methods (Crowley et al., 2002; Peyton and Carrapa, 2013; Fan and Carrapa, 2014; Stevens et al., 2016[[Stevens et al., 2016 is not in the reference list. See suggested reference in Refs Cited.]]). Results indicate that the arches were exhumed in a westward sequence, starting with the Bighorn Mountains (91–57 Ma, rapid phase since 71 Ma), followed by the Wind River Range (90 – 50 Ma, rapid phase since 64 Ma), and finally the Beartooth Mountains (65–54 Ma, rapid phase since 57 Ma) (Fig. 3). The switch from slow to rapid exhumation is interpreted to reflect a transition from flat slab subduction to slab rollback (Fan and Carrapa, 2014).

The stress history has also been extensively documented in the Bighorn Basin, and distinct orientations for Sevier (~N090–110°E) and Laramide (~N040–060°E) compressional stresses (Fig. 2B) were highlighted from microstructural and paleostress analyses (Craddock and Van der Pluijm, 1999; Bellahsen et al., 2006; Neely and Erslev, 2009; Amrouch et al., 2010; Beaudoin et al., 2012; Weil and Yonkee, 2012). A

comprehensive study of the vein network documented across the basin reveals three main systematic vein (opening mode I) sets:

(1) Set S comprises bed-perpendicular veins showing a subvertical attitude and a $N100^{\circ}E \pm 10^{\circ}$ strike after unfolding; they are likely related to layer-parallel shortening in response to Sevier compression.

(2) Set L-I comprises bed-perpendicular, subvertical veins striking $N050^{\circ}E \pm 10^{\circ}E$ that are likely related to layer-parallel shortening during Laramide compression.

(3) Set L-II veins are bed-perpendicular and strike parallel to fold axes ($\sim N135^{\circ}E$), and reflect local extension at fold hinges during Laramide folding (e.g., Bellahsen et al., 2006).

The limited occurrence of set S in the western part of the Bighorn Basin is interpreted as a result of the eastward attenuation of the deformation away from the Sevier orogenic front (Beaudoin et al., 2012), echoing a differential stress magnitude attenuation documented at craton-scale in the Sevier foreland (Van der Pluijm et al., 1997).

METHODS AND RESULTS

Calcite veins belonging to the three different systematic vein sets were collected from Paleozoic limestones and sandstones in the Rattlesnake Mountain, Sheep Mountain–Little Sheep Mountains, and western Bighorn Mountains (Figs. 1 and 2; Table DR1 in the [GSA Data Repository](#)¹). Geochemical analyses showed that the calcite precipitated from a mixture of local seawater and basement-sourced hydrothermal fluids (Barbier et al., 2012, Beaudoin et al., 2014). Textural analysis ensured that calcite crystals precipitated during or soon after vein opening by selection of antitaxial,

elongated blocky or blocky textures (Bons et al., 2012; see the Data Repository). Polished sections were analyzed using laser ablation–inductively coupled plasma–mass spectrometry (LA-ICP-MS) at the [Natural Environment Research Council](#) (NERC) Isotope Geosciences Laboratory (Nottingham, UK) using standard methods for calcite U-Pb geochronology (Roberts and Walker, 2016; Roberts et al., 2017). Ages were determined from Tera-Wasserburg lower intercepts using free regressions, are quoted at 2σ , and include propagation of systematic uncertainties. Twenty-four (24) calcite vein cements yielded reliable age data, with the results presented in Figure 3. Details on the method, full results, and further sample information [can be found in the Data Repository](#).

The U-Pb ages span from 89.7 ± 2.9 to 1.75 ± 0.58 Ma, with MSWD criteria from 0.3 to 52.0, and 19 results having an MSWD <5 (Table DR1). Excluding very young ages (5.56 ± 0.49 to 1.75 ± 0.58 Ma [\[\[no brackets needed here, correct?\]\]](#), $n = 3$) that are not likely to represent the timing of vein development, the range of ages of Set S veins is 75.3 ± 2.8 to 59.5 ± 2.7 Ma ($n = 2$) in the east of the basin and 89.7 ± 2.9 to 45.9 ± 5.3 Ma ($n = 6$) in the west of the basin. The range of ages of L-I veins is 72.0 ± 3.0 to 53.5 ± 1.8 Ma ($n = 6$) in the east and 60.5 ± 4.6 to 34.4 ± 4.1 Ma ($n = 3$) in the west. The range of ages of L-II veins is 45.4 ± 1.8 to 37.2 ± 4.1 Ma ($n = 2$) in Sheep Mountain and 27.9 ± 1.1 to 14.5 ± 0.7 Ma ($n = 2$) in Rattlesnake Mountain.

DISCUSSION AND CONCLUSIONS

U-Pb dating of calcite cements gives an independent assessment of the absolute timing of vein development (Fig. 3). The succession of vein filling U-Pb ages is in line with the deformation sequence inferred from the microstructural approach: Sevier-related S veins predate L-I veins, and L-I veins predate L-II veins, with only a very short overlap

of veins S and L-I at **ca.** 60 Ma. The correlation between the field-based analysis of vein network orientation and overprinting relationships and our absolute vein dating results provides support of both methods as robust means to decipher brittle tectonic histories.

While most U-Pb ages are interpreted to reflect periods of vein opening and fluid precipitation, younger ages suggest that the isotopic signature does not always reflect the time of initial vein filling, despite the absence of any obvious textural evidence for vein re-opening or cement dissolution-reprecipitation. This indicates either that joints may have remained open during a certain time without healing (e.g., S vein aged 45.9 Ma), that veins were tectonically reactivated, or that a resetting of the isotopic system has occurred due to high temperature. Considering the latter mechanism, we suggest that hydrothermal fluid-flow related to extensional/thermal events (Basin and Range, Yellowstone activity) accounts for the veins aged 5–2 Ma. The range of U-Pb ages documented for veins of a given set also suggests a significant duration of the fracturing event, and/or that veins may require variable durations to heal (Becker et al., 2010).


In order to discuss the absolute timing of Sevier and Laramide deformation, we consider the oldest U-Pb ages obtained for each systematic vein set to represent tectonic events at the scale of the basin, with the aim of avoiding ages potentially related to vein rejuvenation. Layer-parallel shortening related to Sevier compression began earlier in the western part of the Bighorn Basin ($90 \text{ Ma} \pm 3 \text{ Ma}$) than in its eastern part ($75 \text{ Ma} \pm 3 \text{ Ma}$). At that time, the future Bighorn Basin was located east of the Sevier orogenic front (Wyoming Salient), so that this age difference can be interpreted as an eastward transmission of Sevier stress and related propagation of layer-parallel shortening in the sedimentary cover. This conclusion is in good agreement with the sequence of Sevier

deformation already proposed (DeCelles, 2004; Solum and van der Pluijm, 2007; Beaudoin et al., 2012; Pană and van der Pluijm, 2015).

Layer-parallel shortening related to Laramide compression started in the east of the Bighorn Basin ($72 \text{ Ma} \pm 3 \text{ Ma}$) before affecting the west ($60.5 \text{ Ma} \pm 3.5 \text{ Ma}$). This westward sequence echoes the exhumation sequence of the Laramide arches inferred from cooling ages (Peyton and Carrapa, 2013; Fan and Carrapa, 2014). However, northeast-directed Laramide layer-parallel shortening initiated in the east of the basin, while Sevier east-directed layer-parallel shortening was still prevailing in the west. This time overlap reflects a spatial stress compartmentalization within the basin that can be linked to an expression of decoupling of the stress prevailing in the basement and the sedimentary cover. Following Erslev's (1993) concept of stress guides proposed for the area, we suggest that the east-directed compression associated with the Sevier thinned deformation was transmitted along a shallow stress guide (the sedimentary cover), while the northeast-directed Laramide compression was instead transmitted eastward through a deep (crustal-lithospheric?) stress guide (Fig. 4). This northeast-directed compression thus caused sequential reactivation of the inherited basement faults (depending on their orientation and weakness). Reactivation of such high-angle reverse faults would have vertically transmitted the northeast-southwest stress from the basement to the overlying (attached) cover, resulting in the development in the cover of vein sets under northeast-southwest stress that follows the sequence of uplift of the basement arches related to basement fault reactivation (Fig. 4).

Laramide folding is dated by the opening of the syn-folding L-II veins, and at basin scale, the U-Pb ages are younger in the west of the Bighorn Basin ($28 \text{ Ma} \pm 3 \text{ Ma}$)

than in the east ($45 \text{ Ma} \pm 3 \text{ Ma}$). The relatively young age of the Laramide syn-folding veins at Rattlesnake Mountain shows that Laramide folding was still active in the Bighorn Basin during the Oligocene, when some major arches were still uplifting (Wind River range; Steidtmann et al., 1989). The new absolute time constraints that we provide on the westward sequence of folding also mimics the sequence of exhumation of the Laramide arches (Fig. 4). This supports the structural interpretation that the Sheep and Rattlesnake Mountain anticlines developed on top of retro-thrusts soled on the crustal-scale thrusts on which arches developed (Bighorn Mountains and Beartooth Range, respectively) (Neely and Erslev, 2009; Weil and Yonkee, 2012).

To conclude, U-Pb direct dating of systematic vein sets in the Bighorn Basin provides absolute time constraints and confirmation of existing structural models for propagation of Sevier orogenic deformation and of exhumation of Laramide basement-cored structures, while helping to refine the sequence of activation of individual basement thrusts, and aiding our understanding of stress transmission at the basin scale. The results support that (1) thin-skinned orogenic wedges develop through a progressive outward (forelandward) stress loading and propagation of the deformation through time; and (2) thick-skinned systems show a more erratic sequence (Lacombe and Bellahsen, 2016) owing to the reactivation of basement heterogeneities that govern the stress field in the overlying sedimentary cover. This study highlights the interest  of the use of U-Pb dating of vein networks for unravelling the sequence of deformation in complex orogenic forelands.

ACKNOWLEDGMENTS

205 We thank reviewers B. van der Pluijm, S. Marshak, and U. Ring, along with
206 editor D. Brown, for their constructive comments. This work was funded by Sorbonne
207 Université (Paris) through research agreement C14313 and the **Natural Environment**
208 **Research Council (UK)** through NIGSFC grant IP-1494–1114.

209 **REFERENCES CITED**

- 210 Amrouch, K., Lacombe, O., Bellahsen, N., Daniel, J.M., and Callot, J.P., 2010, Stress and
211 strain patterns, kinematics and deformation mechanisms in a basement-cored
212 anticline: Sheep Mountain Anticline, Wyoming: *Tectonics*, v. 29, TC1005,
213 <https://doi.org/10.1029/2009TC002525>.
- 214 Barbier, M., Leprêtre, R., Callot, J.-P., Gasparini, M., Daniel, J.-M., Hamon, Y.,
215 Lacombe, O., and Floquet, M., 2012, Impact of fracture stratigraphy on the paleo-
216 hydrogeology of the Madison Limestone in two basement-involved folds in the
217 Bighorn basin, (Wyoming, USA): *Tectonophysics*, v. 576–577, p. 116–132,
218 <https://doi.org/10.1016/j.tecto.2012.06.048>.
- 219 Beaudoin, N., Leprêtre, R., Bellahsen, N., Lacombe, O., Amrouch, K., Callot, J.-P.,
220 Emmanuel, L., and Daniel, J.-M., 2012, Structural and microstructural evolution of
221 the Rattlesnake Mountain Anticline (Wyoming, USA): New insights into the Sevier
222 and Laramide orogenic stress build-up in the Bighorn Basin: *Tectonophysics*,
223 v. 576–577, p. 20–45, <https://doi.org/10.1016/j.tecto.2012.03.036>.
- 224 Beaudoin, N., Bellahsen, N., Lacombe, O., Emmanuel, L., and Pironon, J., 2014, Crustal-
225 scale fluid flow during the tectonic evolution of the Bighorn Basin (Wyoming,
226 USA): *Basin Research*, v. 26, p. 403–435, <https://doi.org/10.1111/bre.12032>.

- 227 Becker, S.P., Eichhubl, P., Laubach, S.E., Reed, R.M., Lander, R.H., and Bodnar, R.J.,
228 2010, A 48 m.y. history of fracture opening, temperature, and fluid pressure:
229 Cretaceous Travis Peak Formation, East Texas basin: Geological Society of America
230 Bulletin, v. 122, p. 1081–1093, <https://doi.org/10.1130/B30067.1>.
- 231 Bellahsen, N., Fiore, P., and Pollard, D.D., 2006, The role of fractures in the structural
232 interpretation of Sheep Mountain Anticline, Wyoming: Journal of Structural
233 Geology, v. 28, p. 850–867, <https://doi.org/10.1016/j.jsg.2006.01.013>.
- 234 Bergbauer, S., and Pollard, D.D., 2004, A new conceptual fold-fracture model including
235 prefolding joints, based on the Emigrant Gap anticline, Wyoming: Geological
236 Society of America Bulletin, v. 116, p. 294, <https://doi.org/10.1130/B25225.1>.
- 237 Bons, P.D., Elburg, M.A., and Gomez-Rivas, E., 2012, A review of the formation of
238 tectonic veins and their microstructures: Journal of Structural Geology, v. 43, p. 33–
239 62, <https://doi.org/10.1016/j.jsg.2012.07.005>.
- 240 Craddock, J.P., and Van der Pluijm, B.A., 1999, Sevier–Laramide deformation of the
241 continental interior from calcite twinning analysis, west-central North America:
242 Tectonophysics, v. 305, p. 275–286, [https://doi.org/10.1016/S0040-1951\(99\)00008-](https://doi.org/10.1016/S0040-1951(99)00008-6)
243 6.
- 244 Crowley, P.D., Reiners, P.W., Reuter, J.M., and Kaye, G.D., 2002, Laramide exhumation
245 of the Bighorn Mountains, Wyoming: An apatite (U-Th)/He thermochronology
246 study: Geology, v. 30, p. 27–30, [https://doi.org/10.1130/0091-](https://doi.org/10.1130/0091-7613(2002)030<0027:LEOTBM>2.0.CO;2)
247 7613(2002)030<0027:LEOTBM>2.0.CO;2.


- 248 DeCelles, P.G., 2004, Late Jurassic to Eocene evolution of the Cordilleran thrust belt and
249 foreland basin system, western USA: *American Journal of Science*, v. 304, p. 105–
250 168, <https://doi.org/10.2475/ajs.304.2.105>.
- 251 Erslev, E.A., 1993, Thrusts, back-thrusts and detachment of Rocky Mountain foreland
252 arches, *in* Schmidt, C.J., et al., eds., *Laramide Basement Deformation in the Rocky*
253 *Mountain Foreland of the Western United States: Geological Society of America*
254 *Special Papers*, v. 280, p. 339–358, <https://doi.org/10.1130/SPE280-p339>.
- 255 Erslev, E.A., and Rogers, J.L., 1993, Basement-cover geometry of Laramide fault-
256 propagation folds, *in* Schmidt, C.J., et al., eds., *Laramide Basement Deformation in*
257 *the Rocky Mountain Foreland of the Western United States: Geological Society of*
258 *America Special Papers*, v. 280, p. 125–146, <https://doi.org/10.1130/SPE280-p125>.
- 259 Fan, M., and Carrapa, B., 2014, Late Cretaceous–early Eocene Laramide uplift,
260 exhumation, and basin subsidence in Wyoming: Crustal responses to flat slab
261 subduction: *Tectonics*, v. 33, p. 509–529, <https://doi.org/10.1002/2012TC003221>.
- 262 Hansman, R.J., Albert, R., Gerdes, A., and Ring, U., 2018, Absolute ages of multiple
263 generations of brittle structures by U-Pb dating of calcite: *Geology*, v. 46, p. 207–
264 210, <https://doi.org/10.1130/G39822.1>.
- 265 Lacombe, O., and Bellahsen, N., 2016, Thick-skinned tectonics and basement-involved
266 fold–thrust belts: insights from selected Cenozoic orogens: *Geological Magazine*,
267 v. 153, p. 763–810, <https://doi.org/10.1017/S0016756816000078>.
- 268 Marshak, S., Karlstrom, K., and Timmons, J.M., 2000, Inversion of Proterozoic
269 extensional faults: An explanation for the pattern of Laramide and Ancestral Rockies

- 270 intracratonic deformation, United States: *Geology*, v. 28, p. 735–738,
271 [https://doi.org/10.1130/0091-7613\(2000\)28<735:IOPEFA>2.0.CO;2](https://doi.org/10.1130/0091-7613(2000)28<735:IOPEFA>2.0.CO;2).
- 272 Neely, T.G., and Erslev, E.A., 2009, The interplay of fold mechanisms and basement
273 weaknesses at the transition between Laramide basement-involved arches, north-
274 central Wyoming, USA: *Journal of Structural Geology*, v. 31, p. 1012–1027,
275 <https://doi.org/10.1016/j.jsg.2009.03.008>.
- 276 Nuriel, P., Weinberger, R., Kylander-Clark, A., Hacker, B., and Craddock, J., 2017, The
277 onset of the Dead Sea transform based on calcite age-strain analyses: *Geology*, v. 45,
278 p. 587–590, <https://doi.org/10.1130/G38903.1>.
- 279 Pană, D.I., and van der Pluijm, B., 2015, Orogenic pulses in the Alberta Rocky
280 Mountains: Radiometric dating of major faults and comparison with the regional
281 tectono-stratigraphic record: *Geological Society of America Bulletin*, v. 127, p. 480–
282 502, <https://doi.org/10.1130/B31069.1>.
- 283 Parrish, R.R., Parrish, C.M., and Lasalle, S., 2018, Vein calcite dating reveals Pyrenean
284 orogen as cause of Paleogene deformation in southern England: *Journal of the*
285 *Geological Society*, v. 175, p. 425–442, <https://doi.org/10.1144/jgs2017-107>.
- 286 Peyton, S.L., and Carrapa, B., 2013, An overview of low-temperature thermochronology
287 in the Rocky Mountains and its application to petroleum system analysis: *AAPG*
288 *Studies in Geology*, v. 65, p. 37–70.
- 289 Ring, U., and Gerdes, A., 2016, Kinematics of the Alpenrhein-Bodensee graben system
290 in the Central Alps: Oligocene/Miocene transtension due to formation of the Western
291 Alps arc: *Tectonics*, v. 35, p. 1367–1391, <https://doi.org/10.1002/2015TC004085>.

- 292 Roberts, N.M., and Walker, R.J., 2016, U-Pb geochronology of calcite-mineralized
293 faults: Absolute timing of rift-related fault events on the northeast Atlantic margin:
294 Geology, v. 44, p. 531–534, <https://doi.org/10.1130/G37868.1>.
- 295 Roberts, N.M., Rasbury, E.T., Parrish, R.R., Smith, C.J., Horstwood, M.S., and Condon,
296 D.J., 2017, A calcite reference material for LA-ICP-MS U-Pb geochronology:
297 Geochemistry Geophysics Geosystems, v. 18, p. 2807–2814,
298 <https://doi.org/10.1002/2016GC006784>.
- 299 Solum, J.G., and van der Pluijm, B.A., 2007, Reconstructing the Snake River – Hoback
300 River Canyon section of the Wyoming thrust belt through direct dating of clay-rich
301 fault rocks, *in* Sears, J.W., et al., eds., Whence the Mountains? Inquiries into the
302 Evolution of Orogenic Systems: A Volume in Honor of Raymond A. Price :
303 Geological Society of America Special Papers, v. 433, p. 183–196.
- 304 Stanton, H.I., and Erslev, E.A., 2004, Sheep Mountain Anticline: Backlimb tightening
305 and sequential deformation in the Bighorn Basin, Wyoming: Wyoming Geological
306 Association Guidebook, v. 53, p. 75–87.
- 307 Stearns, D.W., 1971, Mechanisms of drape folding in the Wyoming province, *in* Renfro,
308 A.R., ed., Symposium on Wyoming Tectonics and Their Economic Significance:
309 Wyoming Geological Association, 23rd Annual Field Conference Guidebook, p.
310 125–143.
- 311 Steidtmann, J.R., Middleton, L.T., and Shuster, M.W., 1989, Post-Laramide (Oligocene)
312 uplift in the Wind River Range, Wyoming: Geology, v. 17, p. 38–41,
313 [https://doi.org/10.1130/0091-7613\(1989\)017<0038:PLOUIT>2.3.CO;2](https://doi.org/10.1130/0091-7613(1989)017<0038:PLOUIT>2.3.CO;2).

- 314 Stevens, A.L., Balgord, E.A., and Carrapa, B., 2016, Revised exhumation history of the
315 Wind River Range, WY, and implications for Laramide tectonics: *Tectonics*, v. 35,
316 p. 1121–1136, <https://doi.org/10.1002/2016TC004126>.
- 317 Stone, D.S., 1993, Basement-involved thrust-generated folds as seismically imaged in the
318 subsurface of the central Rocky Mountain foreland *in* Schmidt, C.J., et al., eds.,
319 Laramide Basement Deformation in the Rocky Mountain Foreland of the Western
320 United States: Geological Society of America Special Papers, v. 280, p. 271–318,
321 <https://doi.org/10.1130/SPE280-p271>.
- 322 Tavani, S., Storti, F., Lacombe, O., Corradetti, A., Muñoz, J.A., and Mazzoli, S., 2015, A
323 review of deformation pattern templates in foreland basin systems and fold-and-
324 thrust belts: Implications for the state of stress in the frontal regions of thrust
325 wedges: *Earth-Science Reviews*, v. 141, p. 82–104,
326 <https://doi.org/10.1016/j.earscirev.2014.11.013>.
- 327 Van der Pluijm, B.A., Craddock, J.P., Graham, B.R., and Harris, J.H., 1997, Paleostress
328 in cratonic North America: Implications for deformation of continental interiors:
329 *Science*, v. 277, p. 794–796, <https://doi.org/10.1126/science.277.5327.794>.
- 330 Weil, A.B., and Yonkee, W.A., 2012, Layer-parallel shortening across the Sevier fold-
331 thrust belt and Laramide foreland of Wyoming: spatial and temporal evolution of a
332 complex geodynamic system: *Earth and Planetary Science Letters*, v. 357–358,
333 p. 405–420, <https://doi.org/10.1016/j.epsl.2012.09.021>.
- 334 Yonkee, W.A., and Weil, A.B., 2015, Tectonic evolution of the Sevier and Laramide
335 belts within the North American Cordillera orogenic system: *Earth-Science Reviews*,
336 v. 150, p. 531–593, <https://doi.org/10.1016/j.earscirev.2015.08.001>.

FIGURE CAPTIONS

Figure 1. A: Simplified map reporting the Sevier and Laramide ranges (Bighorn Basin (Wyoming, USA; after Yonkee and Weil, 2015). B: Geological map of the Bighorn Basin, with location of the studied structures and samples. C: Crustal cross section in the Laramide foreland; dotted red line in A, red line in B (after Marshak et al., 2000; Lacombe and Bellahsen, 2016). BHB—Bighorn Basin, BM—Bighorn Mountains, OC—Owl Creek Mountains, WR—Wind River Mountains, WRB—Wind River Basin, BH—Black Hills, GRB—Green River Basin, PRB—Powder River Basin, LSMA—Little Sheep Mountain anticline, SMA—Sheep Mountain anticline, RMA—Rattlesnake Mountain anticline, BT—Beartooth Mountains, RT—Rio Thrust, OT—Oregon Thrust K—?? —?; J—?. [[Define these]]

[[In figure, panel A, make the label for the rectangle of panel B uppercase, “B”; delete the text label “c”?]]

Figure 2. A; Sketch representing the vein network in the Bighorn Basin (Wyoming, USA). B: Orientation of the main vein sets encountered across the basin, corrected from strata tilting, reported on a lower hemisphere Schmidt stereonet; color code matches A. [[Define LPS (layer-parallel shortening?)]] C: Field photograph illustrating chronological relationship of some fracture sets at Rattlesnake Mountain anticline (RMA). D: Successive orientations of horizontal principal stresses in the Bighorn Basin reconstructed from paleostress analyses (modified after Beaudoin et al., 2014). [[In figure, panel B, close up space in “L- II” for consistency]]

Figure 3. Diagram of U-Pb ages (Ma) of the calcite cements of vein sets versus longitude.

The schematic east-west cross section locates the samples. Right-hand side: ages of exhumation of the basement arches bounding the Bighorn Basin (Wyoming, USA) with slow exhumation in light gray and rapid exhumation in dark gray (after Fan and Carrapa, 2014); in pink are reported the timespan of the Basin and Range extension (B&R) and of activity of the Yellowstone hotspot (YHS). RMA—Rattlesnake Mountain anticline; LSMA—Little Sheep Mountain anticline; SMA—Sheep Mountain anticline; BM—Bighorn Mountains; B&R—Basin and Range; BT—Beartooth Mountains; WR—Wind River Mountains; BM—Bighorn Mountains. **[[Define LPS]]**

[[In figure, left axis, change U/Pb to U-Pb;

Figure 4. Evolution of thrust activation along a schematic W/SW–E/NE cross section of the Bighorn Basin (Wyoming, USA). Laramide stress overprint in the cover is reported as a gray shade. Activation of basement faults is symbolized by a red plane, and ages are inferred from published thermochronological data for the arch uplift and exhumation (noted *), and from U-Pb ages for the basin interior. **[[BHM—Bighorn Mountains?, If so, use consistent terminology; e.g., BM]].** BT—Beartooth Mountains; RMA—Rattlesnake Mountain anticline; BT—Beartooth Mountains; SMA—Sheep Mountain anticline.

[[In figure, use hyphens or dashes consistently in age ranges.]]

¹GSA Data Repository item 2018xxx, **[[Provide DR item names and brief descriptions here]]**, is available online at

383 <http://www.geosociety.org/datarepository/2018/>, or on request from

384 editing@geosociety.org.